Electrochimica Acta 329 (2020) 135177

Contents lists available at ScienceDirect

Electrochimica Acta

journal homepage: www.elsevier.com/locate/electacta

Nanoporous Cu_2O nanotube/nanorod array electrodes for non-enzymatic glucose sensing with high sensitivity and very low detection limit

Lakmini Jayasingha [a], Charith Jayathilaka [b], Roshantha Kumara [c], Koji Ohara [c], Migelhewa Kaumal [d], Siyath Gunewardene [a], Dhammike Dissanayake [d], Sumedha Jayanetti [a, e, *]

[a] Department of Physics, University of Colombo, Colombo 03, Sri Lanka
[b] Department of Physics, University of Kelaniya, Kelaniya, Sri Lanka
[c] Research & Utilization Division, Japan Synchrotron Radiation Research Institute (JASRI), 1-1-1, Kouto, Sayo- cho, Sayo-gun, Hyogo, 679-5198, Japan
[d] Department of Chemistry, University of Colombo, Colombo 03, Sri Lanka
[e] Department of Instrumentation & Automation Technology, University of Colombo, Colombo 03, Sri Lanka

ARTICLE INFO

Article history:
Received 7 March 2019
Received in revised form
7 June 2019
Accepted 29 October 2019
Available online 2 November 2019

Keywords:
Electrochemical anodization
Nanoporous Cu_2O nanotubes/nanorods · chronoamperometry
Sensitivity
Detection limit

ABSTRACT

This study compares the non-enzymatic glucose sensing performance by Cu_2O nanorods/nanotubes grown using electrochemically anodized Cu foam and Cu plates to form binder free one-dimensional $Cu(OH)_2$ nanostructures which were subsequently annealed at higher temperatures. Resulting Cu_2O nanorods/nanotubes had diameters between 100 and 200 nm and lengths in excess of 10 μm. The surface morphology and structure of these thin films studied using scanning electron microscopy, X-ray diffraction and energy dispersive X-ray spectroscopy showed that the copper foam based Cu_2O structures consisted of nanotubes/nanorods distributed over entire 3-dimensional space containing dense nanopores of size ~20 nm on outer surfaces. Cu plate based nanorods consisted of grooved macaroni type surface morphologies. Non-enzymatic glucose sensing made using chronoamperometric and cyclic voltammetric measurements showed that the Cu_2O/Cu foam electrodes had a high sensitivity of 5792.7 μA mM^{-1} cm^{-2}, a very low detection limit of 15 nM (S/N = 3), multi-linear detection ranges of 15 nM–0.1 μM and 575–4098.9 μM with a faster response time of less than 1 s. Cu plate based nanorods showed a sensitivity of 141.9 μA mM^{-1} cm^{-2}, with a lower detection limit of 510 nM (S/N = 3). The significantly high sensitivity of Cu_2O/Cu foam electrodes is attributed to the availability of increased amount of active sites due to the large effective surface area provided by Cu_2O nanorods/nanotubes. The study also demonstrates the influence of the substrate on surface morphology of the nanorods/nanotubes. These Cu foam based Cu_2O electrodes provide a promising platform for non-enzymatic glucose detection with high specificity and reproducibility.

1. Introduction

Tunable morphological and electrocatalytic properties of the nanoscale oxide semiconducting materials have led to the construction of miniaturized sensing devices at nanoscale including glucose sensors [1,2]. Although enzymatic glucose sensors are characterized with high glucose selectivity, they suffer deactivation due to long time storage and on exposure to elevated temperatures. Therefore, there is renewed interest on the development of highly sensitive, reproducible, and robust not-enzymatic glucose sensors. Many metals (Au [3], Pt [4], Cu [5,6] etc.) and metal oxides (ZnO [7–9], TiO_2 [10], Co_3O_4 [11,12]), and CuO [13–15] have been investigated in this regard. Among them copper oxide based sensors have received much attention due to ease of fabrication and low cost, and non-toxicity [16,17]. In recent times, interests have arisen towards the development of transition metal oxide nanostructures in one-dimension (1D). Investigations

* Corresponding author. Department of Physics, University of Colombo, Colombo 03, Sri Lanka.
E-mail address: sumedha@phys.cmb.ac.lk (S. Jayanetti).

https://doi.org/10.1016/j.electacta.2019.135177
0013-4686/

on such nanostructured electrodes have opened paths to optimize the mass and charge transport properties and electron transfer kinetics [12,18]. On the other hand, Faradaic currents associated with kinetically controlled electrochemical processes depend on the real surface area of an electrode, rather than its geometric area. Therefore, electrodes with high surface area can be used to enhance selectively the Faradaic current of a kinetically controlled electrochemical reaction [19]. Moreover, electrochemical reactions between the interface of electrolyte and surface of the electrode, ionic movements between the electrodes and current collector (substrate) are essential to enhance the electronic conductivity. In the development of electrodes with morphological structures such as 1D nanostructures: nanowires (NWs), nanotubes (NTs), and nanorods (NRs), Cu_2O has become an attractive material [20,21]. It also has the potential to be one of the best materials for the development of glucose sensors due to its inherent properties such as excellent electro-catalytic activity and electron transfer ability.

In this article, investigation of non-enzymatic glucose detection by the combination of 1D nanoporous nanorod/nanotube (NR/NT) arrays of Cu_2O grown on 3D structured Cu foam (CF) and grooved macaroni type Cu_2O nanorods grown on Cu plates following facile and simpler *in-situ* electrochemical technique is discussed. The deposition method was free of the usage of co-casted polymer binders such as Nafion or polyvinylidene fluoride (PVDF) to form a matrix film from the substances and make the connections between substances and the current collector. These binders affect negatively on performance of sensors. Moreover, polymer binders introduce additional cost. Therefore, synthesis of Cu_2O nanowires by *in-situ* direct etching from conducting Cu substrate in different electrolytes offers a convenient path for sensor electrode construction. Recently, Gao et al. [1] have synthesized mesocrystalline Cu_2O hollow nanocubes with sensitivity of 52.5 $\mu A\,mM^{-1}$ and a lower detection limit (LOD) of 0.87 μM for glucose. Dong et al. [18] have reported ultrahigh sensitivity and ultralow detection limit of 97.9 $mA\,mM^{-1}\,cm^{-2}$ and 5 nM respectively for CF supported Cu_2O nanothorn arrays. Cu_2O pod-like NWs on CFs have been grown using NaOH electrolyte by Lu et al. [17]. They have reported sensitivities as high as 6680.7 $\mu A\,mM^{-1}\,cm^{-2}$ and LOD of 0.67 μM. Li et al. have reported a sensitivity of 2217.4 $mA\,mM^{-1}\,cm^{-2}$ and a lower detection limit of 300 nM for non-enzymatic glucose detection using CuO nanowires grown on CF via anodization [22]. Yu et al. have developed arrays of $CuO/Cu_2O@CuO/Cu_2O$ core-shell nanowires for non-enzymatic glucose detection with ultra-high sensitivity, low detection limit and wide linear range of 10,090 $\mu A\,mM^{-1}cm^{-2}$, 480 nM and 0.99 μM - 1330 μM respectively [23]. CuO nanoneedles modified Graphene/Carbon nanofibers/GCE electrode have been modified by Ye et al. for the detection of glucose, and have reported a sensitivity of 912.7 $\mu A\ mM^{-1}cm^{-2}$ and a low detection limit of 100 nM [15]. Xu et al. have grown CuO nanotube arrays using electrochemical anodization for non-enzymatic glucose sensing applications and reported a sensitivity and a linear detection range of 1890 $\mu A\ mM^{-1}cm^{-2}$ and 5 μM to 3.0 mM respectively [24]. In this study, we report performance of CF supported 1D Cu_2O nanostructures containing a mixture of Cu_2O, NRs and NTs synthesized via electrochemical anodization in a NaOH electrolyte and used as electrodes in glucose sensing using Chronoamperometry. This performance shows a remarkable improvement compared to Cu_2O nanorod electrodes fabricated using electrochemically anodized Cu plates. Therefore, the reported CF based Cu_2O nanoporous sensors may be useful to sense glucose, not only in blood but also in interstitial and adipose tissue, in tears and in glucose based fuel cells.

2. Experimental

2.1. Fabrication of one dimensional nanostructures

Initially, fabrication of 1D $Cu(OH)_2$ nanostructures was accomplished using Hokuto-Denko-Potentiostat/Galvanostat-HA30. The counter electrode was a Pt sheet and the working electrodes were CF (Sigma Aldrich, purity - 99.9% and thickness - 2 mm) or Cu plate (Sigma Aldrich, purity - 99.9%, area - 2 cm × 1 cm and thickness − 0.1 mm). All solutions were prepared using de-ionized water and anodization was performed in an alkaline medium. Prior to the anodization, CFs and Cu plates were ultrasonically cleaned in acetone, ethanol and finally in de-ionized water, each for 10 min. The films were subsequently dried at 60 °C in a dry air stream for a few minutes. The anodization of CFs were carried out in an electrolytic bath containing 3 M NaOH (Sigma−Aldrich, purity ≥ 98.0%) at a bath temperature of 25 °C without stirring. Prior to the anodization, the solution was degassed by ultra-sonication for 15 min at a frequency of 40 kHz. Some experimental information for materials growth were adapted from Li et al. [22]. The applied current density was 10 $mA\,cm^{-2}$ and anodization times were, 30 min for CF and 10 min for Cu plates. After anodization, the samples were thoroughly washed in de-ionized water several times and dried in a dry air stream at 100 °C for 5 min. Prepared $Cu(OH)_2$ (blue color) nanostructures on CFs and Cu plates were converted to Cu_2O (dark brown) by keeping in a controlled N_2 atmosphere at 180 °C for 1 h and then 500 °C for 3 h in a tube furnace (ISUZU Micro Computer Controller). The films were then allowed to naturally cool down to room temperature.

2.2. Materials characterization

Zeiss Evols15 scanning electron microscope (SEM) was used to analyze the morphology of the samples. The crystalline structure of the deposited films were studied with X-ray diffractometry (XRD) (Shimadzu (XD-D1)) using Cu-Kα ($\lambda = 1.542$ A) as the source of X-rays. The scan rate was 2° min^{-1}. In addition, High-energy X-ray diffraction (HEXRD) measurements were obtained at room temperature with incident photon energy of 61.37 keV and wavelength of 0.202 Å, at the BL04B2 beamline of the 8 GeV synchrotron radiation facility SPring-8, Hyogo, Japan. Data were collected using four CdTe detectors and two Ge detectors in step scan mode at a scan rate of 0.1° s^{-1} for the scan angle region from 0.3° to 17° to cover a scattering angle from 0.3° to 45°. Samples for x-ray diffraction were prepared by peeling off the Cu_2O films from the substrates and packing them in silica capillaries having dimensions of 1 mm ID × 0.2 mm t × 70 mm length.

2.3. Electrochemical characterization

Cyclic voltammetric (CV) and Chronoamperometry (CA) techniques were performed using Ziew SP5 electrochemical workstation to study the electrochemical kinetic properties of the electrodes. Reference and counter electrodes were Ag/AgCl and a Pt sheet respectively. CV measurements were also utilized to determine the active microscopic surface area using Randle's-Servcik equation. All the measurements were made at room temperature (25 °C).

3. Results and discussion

3.1. Materials characterization

Increasing temperature up to 180 °C for 1 h and then further increasing up to 500 °C for 3 h anodized $Cu(OH)_2$ structures

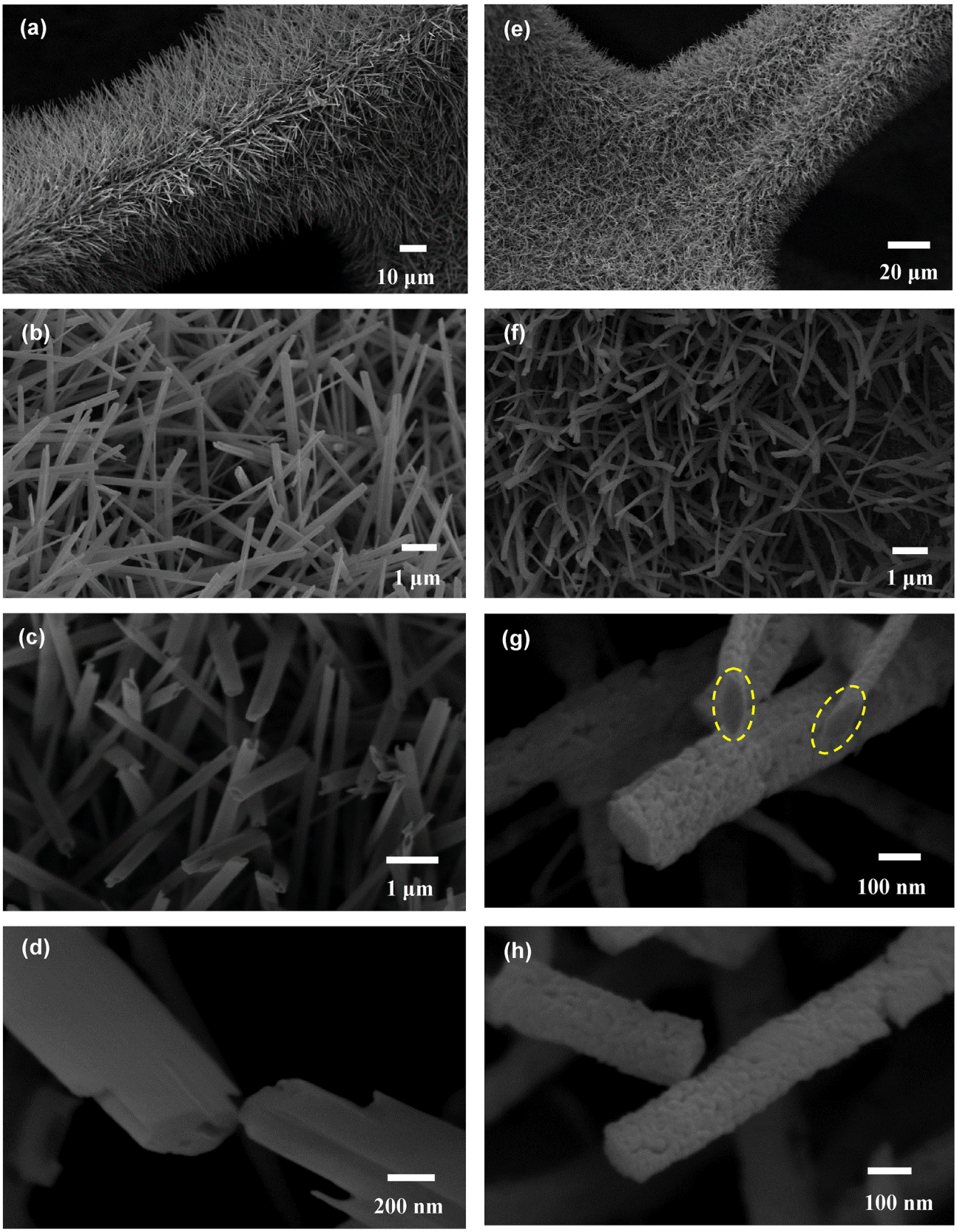

Fig. 1. SEM images at different magnifications of (a)–(d) - $Cu(OH)_2$ film grown on Cu Foam after anodization in a 3 M NaOH solution by applying a current density of 10 mA cm^{-2} at 25 °C for 30 min and (e)–(h) nanoporous mixed-structures of Cu_2O nanotubes/nanorods at different magnifications, after annealing of $Cu(OH)_2$ thin films under N_2 atmosphere at 180 °C for 1 h and 500 °C for 3 h. Yellow circles indicate the tube facets with outer diameters around 100 nm.

transform into Cu_2O nanostructures. The decomposition follows the sequence; $Cu(OH)_2 \rightarrow CuO \rightarrow Cu_2O$ and the conversion of $Cu(OH)_2$ to CuO corresponds to dehydration in a N_2 gas atmosphere. Fig. S1 shows the SEM images of CF substrates at different magnifications. It can be seen that CF has a honeycomb-like 3-dimensional (3D) structure (Fig. S1 (a)), that provides a large area for surface reactions [18]. *In-situ* structural evolution from $Cu(OH)_2$ nanostructures to Cu_2O nanostructures grown on CF and Cu plates were studied by SEMs. As can be seen in Fig. 1(a)–(d), arrays of straight $Cu(OH)_2$ NRs/NTs are formed on CF in an *in-situ* electrochemical anodization process in a 3 M NaOH solution at 25 °C for 30 min. These nano-structured $Cu(OH)_2$ arrays have dimensions of length more than 10 μm and the diameters in the range ~ 100–300 nm. As can be observed in SEM images taken at different magnifications (Fig. 1(e)–(h)). Fig. 1 (f) shows that the Cu_2O nanostructures had lost the straight upright nature observed in the $Cu(OH)_2$ nanostructures. It is also noteworthy to observe the highly porous nature of the Cu_2O surfaces with structures shrinking to have diameters in the range 100–200 nm (Fig. 1(g) and (h)) compared to the $Cu(OH)_2$ nanostructures shown in Fig. 1 (d). Also, resulting Cu_2O nanostrucutres have both nanotubular and nanorod type configurations with nano-pores (Fig. 1(g) and (h)) of sizes around 20 nm on outer surfaces. Sahoo et al. who have reported the growth of a mixture of Cu_2O nanostructures on different areas on SiO_2/Si substrates via anodization [25].

Fig. 2 shows $Cu(OH)_2$ and Cu_2O nanostructured thin films grown on Cu plates. Initially formed $Cu(OH)_2$ NRs on Cu plate through electrochemical anodization by applying 10 mA cm^{-2} in a 3 M sodium hydroxide solution for 10 min can be seen in Fig. 2(a)–(d). Morphology characterized by SEM revealed that the diameters of the NR structures were in the range from 100 nm to 200 nm with lengths exceeding 1 μm (Fig. 2(a) and (b)). Fig. 2(c) and (d) show the Cu_2O NRs formed by repeating the annealing process applied to obtain CF based Cu_2O nanostructures. The surface morphology of the resulting Cu_2O NRs resemble grooved macaroni (rigatoni) type features on their outer surfaces. This shows the effect of substrates (geometry) that has on surface morphology of Cu_2O nano structures during anodization. A comparison of the two morphologies show that the Cu_2O NRs/NTs grown on CF have a very large surface area compared to the Cu_2O NRs grown on Cu plates. Literature reports both Cu_2O and CuO NWs obtained using different fabrication techniques. Wang and co-workers have successfully synthesized crystalline CuO and Cu_2O NWs with an average diameter of about 10 nm and lengths of several tens of microns using $Cu(OH)_2$ NWs as templates [26]. Also, single crystalline Cu_2O NWs have been grown through facile, solution-phase route by Tan et al. [27]. The diameters of the Cu_2O NWs were 40–70 nm and uniform in length. Li-Xu and co-workers have reported the growth of CuO NTs following electrochemical anodization on a copper plate. The reported average diameter and the length of the CuO NTs were about 300 nm and 10 μm, respectively [24].

Fig. 3(a) and (b) show the Laboratory XRD and HEXRD patterns obtained for Cu_2O nanostructures grown on CF. It can be seen that the laboratory XRD pattern shows no impurity peaks (Fig. 3 (a)). In the HEXRD pattern shown in Fig. 3 (b), peaks of very low intensity arising from the CuO phase can be observed. The comparison of the peak strengths are indicative that the samples are essentially due to formation of polycrystalline Cu_2O phase. Fig. S2 (a) and (b) show the HEXRD patterns for Cu_2O NRs grown on Cu plate. Even though weakly intense CuO peaks exist, comparison of the peak strengths with Cu_2O peaks indicates that the samples grown on Cu plate also contain essentially the polycrystalline Cu_2O phase.

3.2. Cyclic voltammetry measurements

The CV measurements were performed to study the

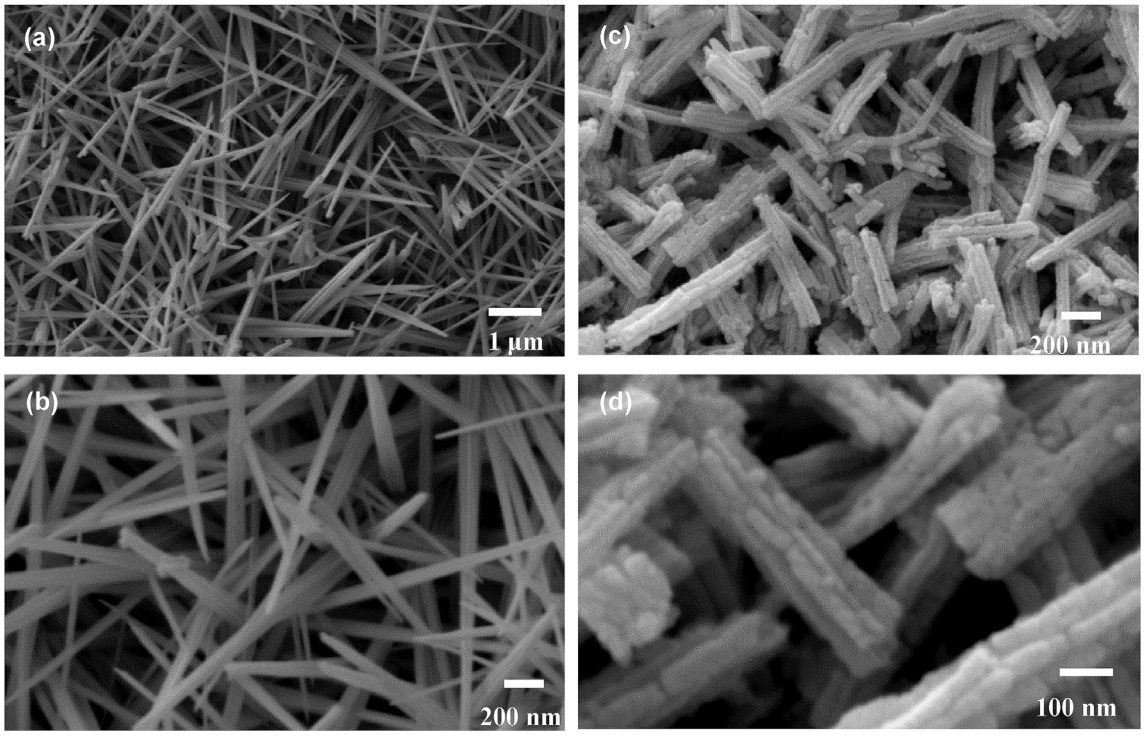

Fig. 2. (a) and (b) - scanning electron microscopic images of $Cu(OH)_2$ nanorods at different magnifications and (c) and (d) - Cu_2O nanorods (at different magnifications) obtained after annealing of $Cu(OH)_2$ thin films under N_2 atmosphere at 500 °C for 3 h..

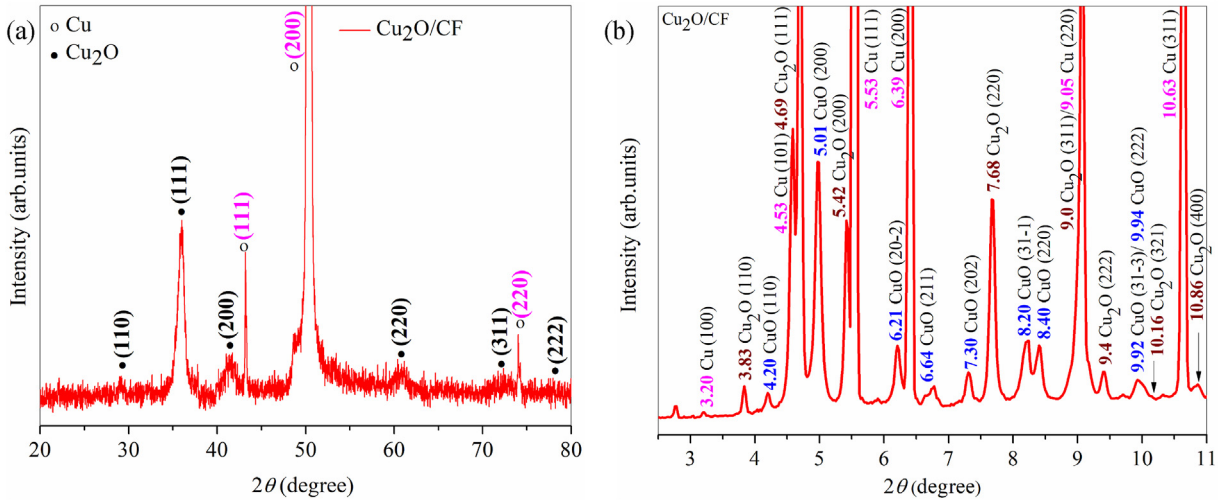

Fig. 3. (a) - Laboratory XRD pattern (λ = 1.54 Å) of Cu_2O nanostructures grown on Copper foam (○ corresponds to Cu peaks and, • corresponds to Cu_2O peaks) (b) - The enlarged pattern of HEXRD measurements (λ = 0.202 Å) obtained for Cu_2O nanostructures grown on copper foam.

electrochemical behavior of the bare Cu_2O/CF, and Cu_2O/Cu plate electrodes in a 0.1 M NaOH solution under the potential range from −0.2 V to +1.0 V vs. Ag/AgCl. Fig. 4 (a) shows the CVs of Cu_2O/CF electrode in the absence (black solid lines) and presence (red solid lines) of 3 mM glucose. It also shows that enhanced current in the presence of glucose occurs throughout the oxidation potential range corresponding to the different oxidation states of Cu. A peak and a shoulder in the absence of glucose were observed with the increase of scan potential from −0.2 V to +1.0 V. The peak at −0.12 V and the shoulder at +0.59 V correspond to the conversion of Cu(I)/Cu(II) and Cu(II)/Cu(III) respectively. Generally, it is believed that the formation of Cu(III) is initialized around +0.6 V [28,29]. However, that peak would be very weak and it is attributed to the use of the low concentration of the alkaline solution (0.1 M NaOH) [30]. Next, the rapid increase of anodic current was observed after the potential reached approximately +0.60 V due to the oxidation of water. Similar results have been observed by Gong et al. for the non-enzymatic glucose oxidation on porous copper@carbon agglomerates [31]. The reduction peak at +0.59 V can be attributed to the conversion of Cu(III)/Cu(II) [31]. In the presence of glucose, oxidation of glucose started from around +0.4 V. At +0.6 V, the increased oxidation current can be attributed to the electro-oxidation of glucose. As shown in Fig. 4 (b), clear redox peaks cannot be observed in the absence of glucose. However, in the presence of 1 mM glucose, the oxidation shoulder appears around +0.5 V.

Fig. 5 shows the CVs of Cu_2O/CF at different glucose concentrations. Obviously, it shows that with the increase in glucose concentration from 0 mM to 6 mM, the anodic oxidation current regularly increases, while the cathodic reduction current decreases suggesting the excellent electrocatalytic properties of Cu_2O/CF electrodes towards the glucose oxidation. The electrocatalytic oxidation process of glucose proceeds in several steps as shown in the following reaction mechanism (Equations (3)–(5)) [17,32]. In an alkaline medium, CuO electrochemically oxidized into highly oxidizing species of Cu(III) such as CuOOH. Glucose is catalytically oxidized into hydrolysate gluconic acid by the Cu(III) species.

$$Cu_2O + 2\,OH^- \rightarrow 2\,CuO + H_2O + 2\,e^- \quad (3)$$

$$CuO + OH^- \rightarrow CuOOH + e^- \quad (4)$$

$$C_6H_{12}O_6 + 2\,CuOOH \rightarrow C_6H_{12}O_7 + 2\,CuO + H_2O \quad (5)$$

The microscopic effective surface areas for Cu_2O/CF electrode and Cu_2O/Cu plate electrode that were estimated using the Randle's Servcik equation [18] were found to be ~0.52 cm^2 and ~0.14 cm^2 respectively. The electro-oxidation of 1 mM glucose on the nanoporous 1D Cu_2O/CF electrode in 0.1 M NaOH solution was studied by varying the scan rate from 50 to 250 mV s^{-1}. Fig. 6 shows the CVs obtained at different scan rates of 50, 75, 100, 125, 150, 175, 200, 225 and 250 mV s^{-1} with the addition of 1 mM glucose to a 0.1 M NaOH (30 ml) solution for Cu_2O/CF and Cu_2O/Cu plate electrodes respectively. It can be seen that, with increasing scan rate, both oxidation and reduction peak currents were increased. Moreover, for Cu_2O/CF electrode, the reduction peak current has shifted towards the more negative region, suggesting a quasi-reversible electron transfer reaction. A Similar observation has been made for glucose oxidation by Cu_2O nanothorn electrodes by Dong et al. [18]. As seen in Fig. 6(c) and (d), both oxidation and reduction currents obtained around +0.5 V vs. Ag/AgCl are directly proportional to the square root of scan rates. This shows that the redox reactions on nanoporous Cu_2O/CF and Cu_2O/Cu plate electrodes are diffusion-controlled electrochemical processes [17]. The regression equations between the peak current and square root of the scan rate can be expressed by equations (6)–(9) given below.

For Cu_2O/CF electrodes:

$$I_{pa}\,(mA) = (0.293 \pm 0.005) \times V^{1/2}\,(mV\ s^{-1})^{1/2} - (1.051 \pm 0.061),\ R^2 = 0.997 \quad (6)$$

$$I_{pc}\,(mA) = (-0.495 \pm 0.012) \times V^{1/2}\,(mV\ s^{-1})^{1/2} + (2.731 \pm 0.142),\ R^2 = 0.996 \quad (7)$$

For Cu_2O/Cu plate electrodes:

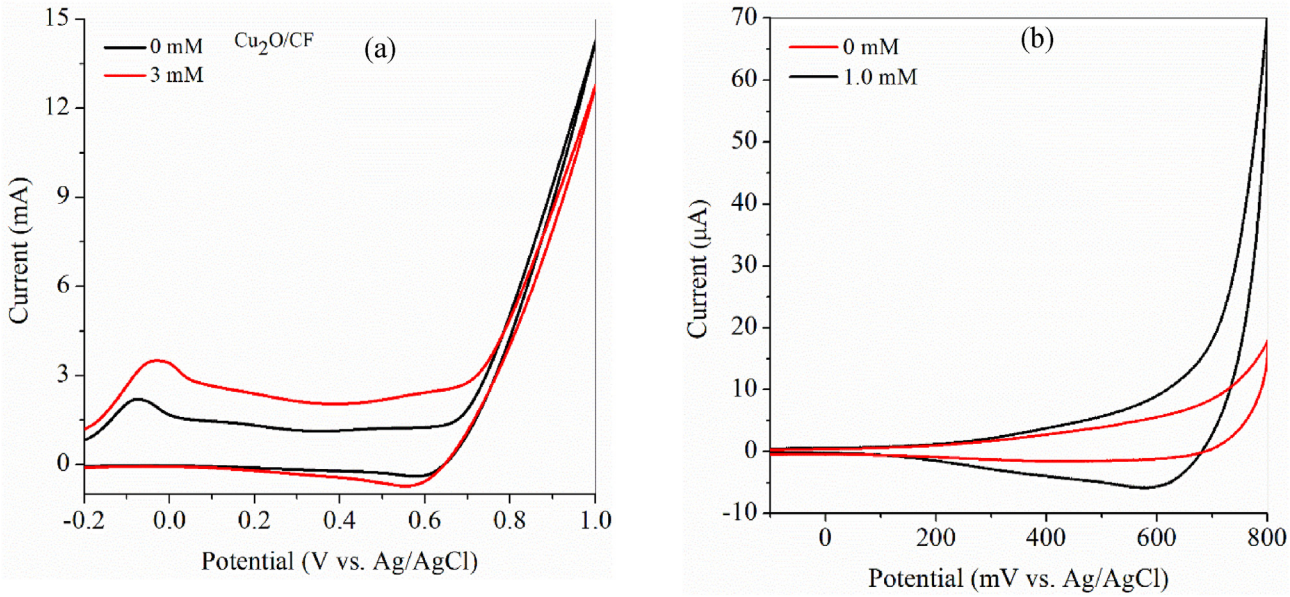

Fig. 4. Cyclic voltammograms of (a) Cu_2O/CF and (b) Cu_2O/Cu plate electrodes in the absence and presence of 3 mM and 1 mM glucose in a 0.1 M NaOH solution.

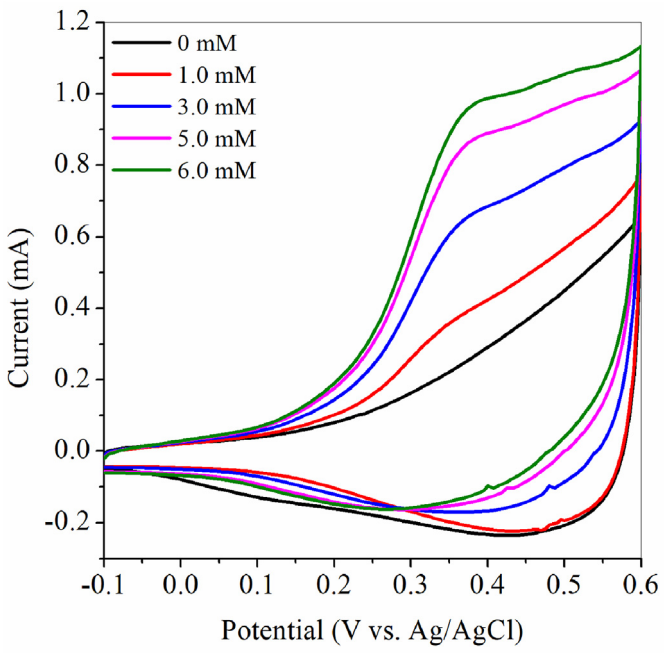

Fig. 5. Cyclic voltammograms of Cu_2O/CF electrode in a 0.1 M NaOH solution with successive addition of glucose with the concentrations of 0 mM, 1 mM, 2 mM, 3 mM, 5 mM and 6 mM. The applied scan rate was 25 mV s^{-1}.

$$I_{pa}\,(\mu A) = \left(4.149 \pm 0.231\right) \times V^{1/2}\left(mV\ s^{-1}\right)^{1/2} - \left(18.152 \pm 2.743\right),\ R^2 = 0.978 \quad (8)$$

$$I_{pc}\,(\mu A) = \left(-4.148 \pm 0.128\right) \times V^{1/2}\left(mV\ s^{-1}\right)^{1/2} + \left(28.022 \pm 1.519\right),\ R^2 = 0.993 \quad (9)$$

3.3. Chronoamperometric measurements

Chronoamperometric measurements were accomplished with successive addition of glucose into the electrolyte with continuous stirring under the applied potential of +0.4 V vs. Ag/AgCl. Fig. 7 (a) shows the amperometric response of Cu_2O/CF electrode of step-like increase of current with successive addition of 0.02 mM, 0.5 mM and 5.0 mM glucose into a 0.1 M NaOH solution. The nanoporous 1D Cu_2O structured electrode (Cu_2O/CF) shows multi-linear detection ranges (up to 0.1 mM) and (575 μM–4098.9 μM) and the high sensitivities of 5792.7 μA mM^{-1} cm^{-2} and 1002.1 μA mM^{-1} cm^{-2} respectively (Fig. 7(b) and (c)). As seen in Fig. 7 (c) (an enlarged section of Fig. 7 (b)) the corresponding linear regression equations can be represented by equations (10) and (11).

$$I\left(mA\right) = \left(3.012 \pm 0.058\right) \times C\left(mM\right) + \left(0.091 \pm 0.004\right),\ R^2 = 0.998 \quad (10)$$

$$I\left(mA\right) = \left(0.521 \pm 0.012\right) \times C\left(mM\right) + \left(0.395 \pm 0.031\right),\ R^2 = 0.996 \quad (11)$$

The current produced from the glucose oxidation, gradually reaches a steady state with increasing glucose concentration. For a comparison, Fig. S3 shows the chronoamperometric response and the corresponding calibration curve on Cu_2O/Cu plate electrode with successive addition of 0.1 mM and 1.0 mM glucose in a 0.1 M NaOH solution at +0.4 V vs. Ag/AgCl. For Cu_2O/Cu plate electrode, the wide linear range of 27 μM–17,280 μM was observed and the sensitivity was only 141.9 μA mM^{-1} cm^{-2}. The corresponding linear regression equation of Cu_2O/Cu plate electrode is as follows (Equation (12)).

$$I(\mu A) = (20.687 \pm 0.166) \times C(mM) + (10.917 \pm 1.551) \quad (12)$$

The sensitivity of Cu_2O/CF electrode is ~41-fold larger than the

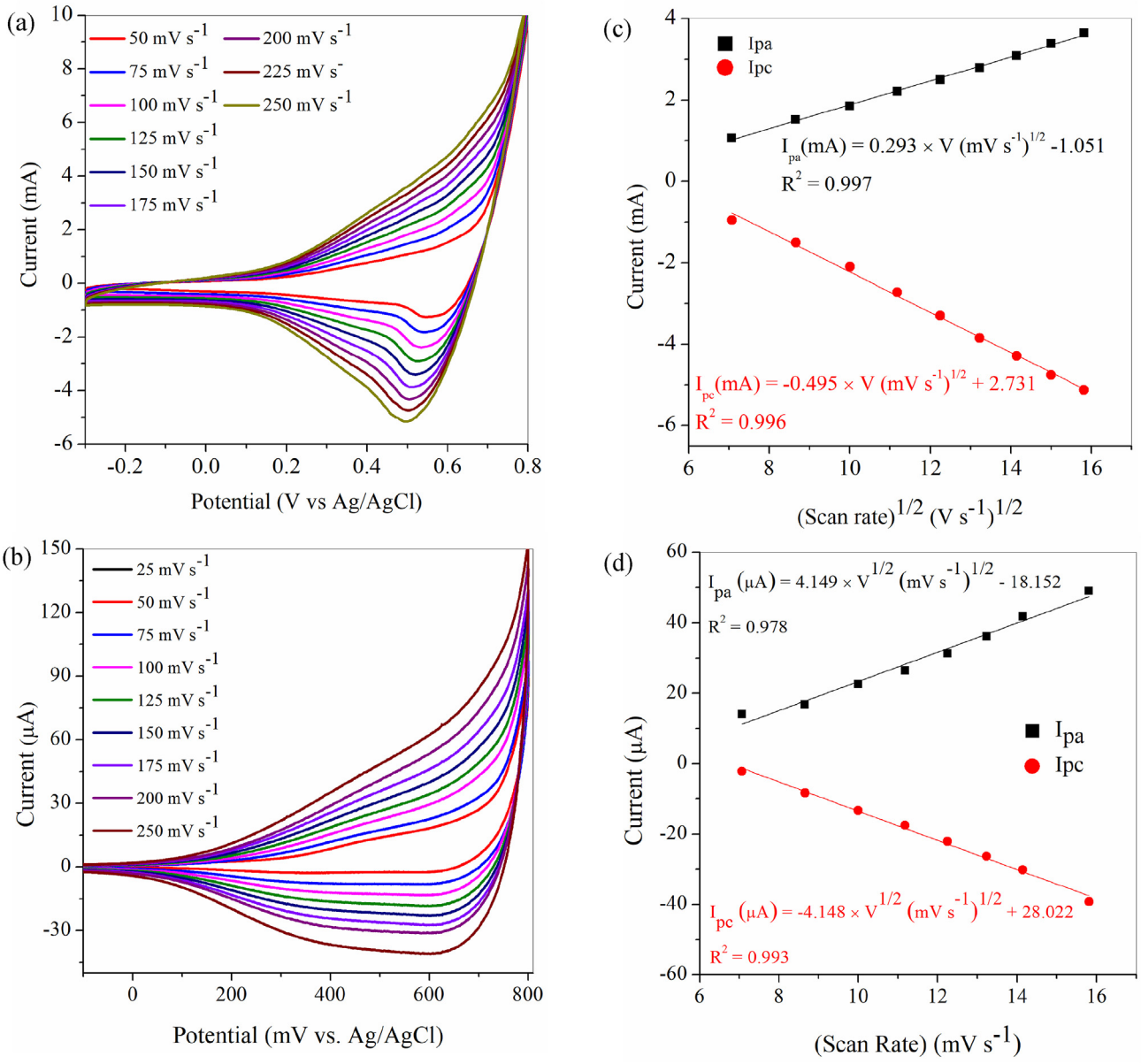

Fig. 6. (a) and (b) - Cyclic voltammograms of Cu_2O/CF and Cu_2O/Cu plate electrodes at different scan rates from 50 to 250 mV s^{-1} in a 0.1 M NaOH solution in the presence of 1 mM glucose. (c) and (d) - the corresponding plots of anodic and cathodic peak currents vs. (scan rate) ^{½} of (a) and (b) respectively.

sensitivity of the Cu_2O/Cu plate electrode. This sensitivity is extremely larger when compared with the sensitivity (490 μA mM^{-1}) reported for CuO/Cu plate [14], 2217.4 μA mM^{-1} cm^{-2} for CuO nanowires [22]. Furthermore, detailed performance of numerous electrodes are summarized in Table 1.

The Langmuir isothermal theory can be used to fit the calibration curve (Fig. 7 (b)) since electrochemical oxidation of glucose on the electrode is a surface catalytic reaction [18]. According to the glucose oxidation, the Langmuir isotherm relationship can be ascribed as follows. The current produced from the glucose oxidation (i_t) is proportional to the concentration of glucose on the material's surface (C_{gs}). Therefore $i_t = K_b\ C_{gs}$, where K_b is the adsorption constant. The sensitivity of the calibration curve can be written as $(S) = di_t/dC_g$. Then, according to the Langmuir theory, the glucose concentration of the surface can be derived as in equation (13) where, C_a is the concentration of active sites on the surface (mol cm^{-2}), C_g is the concentration of the bulk glucose solution (mol cm^{-3}), K_a is the ratio between the adsorption rate constant to the desorption rate constant.

$$C_{gs} = \frac{K_a C_g C_a}{1 + K_a C_g} \tag{13}$$

$$Then: i_t = \frac{K_b K_a C_g C_a}{1 + K_a C_g} \tag{14}$$

$$Therefore: S = \frac{di_t}{dC_g} = \frac{K_b K_a C_a}{(1 + K_a C_g)^2} \tag{15}$$

$$I\ (mA) = \frac{(0.814 \pm 0.024)\ \times\ C(mM)}{1 + (0.055 \pm 0.002)\ \times\ C(mM)}, R^2 = 0.998 \tag{16}$$

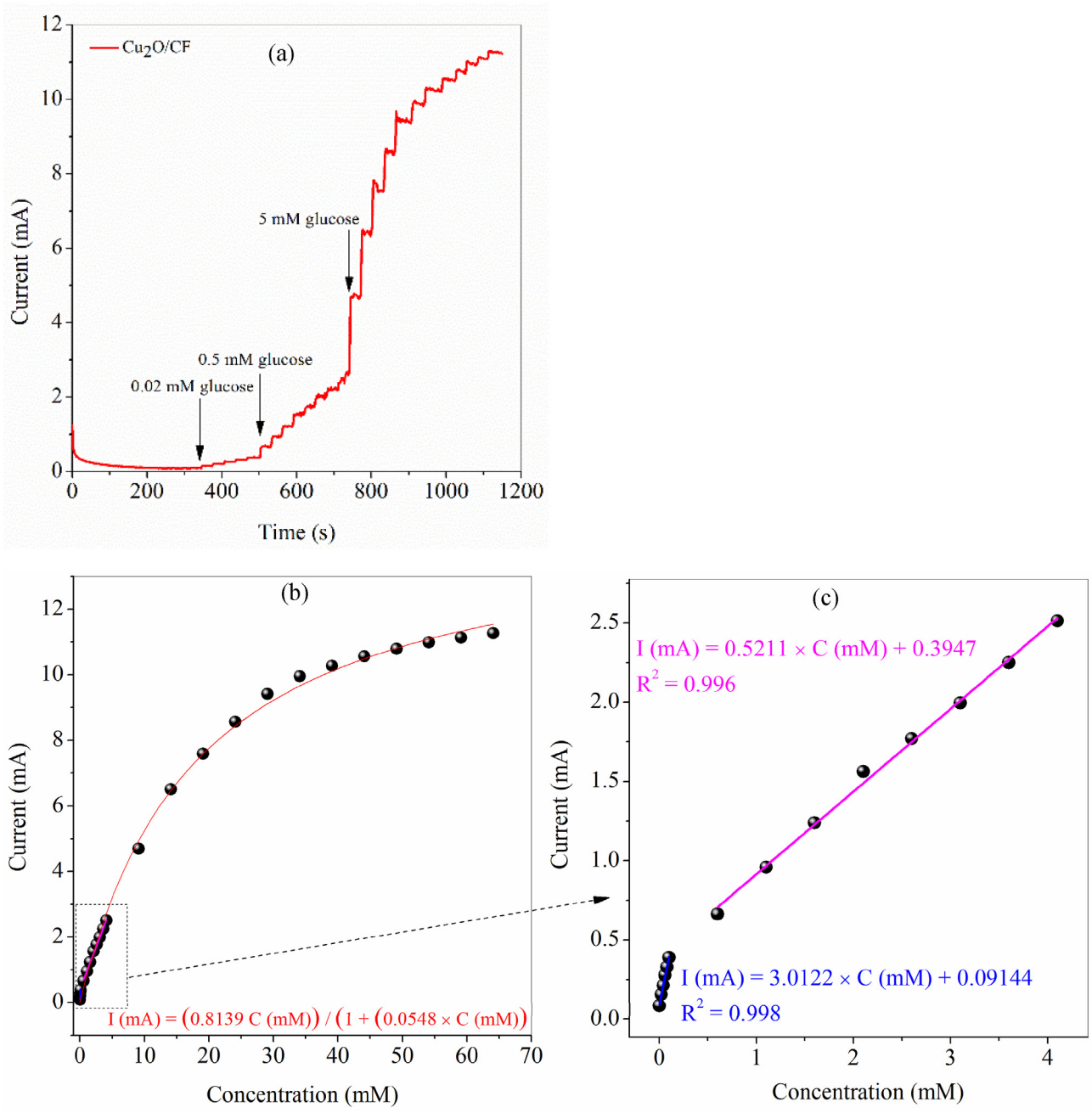

Fig. 7. Chronoamperometric measurements performed on nanoporous Cu_2O nanostructured electrode in a 0.1 M NaOH solution, (a) - with successive additions of different glucose solutions having concentrations of 0.02, 0.5, 5.0 mM at the applied potential of +0.4 V, (b) - the corresponding calibration curve, (c) - an enlarged view of a section of (b).

This yielded a wide detection range up to 60 mM and high sensitivity for the nanoporous 3D Cu_2O/CF electrode with a high correlation coefficient of $R^2 = 0.998$. As C_g is very much lower (1 μM), the sensitivity can be derived from Equation (16) to be 1565.2 μA mM^{-1} cm^{-2}.

Fig. 8 (a) shows the chronoamperometric response of Cu_2O/CF electrode with the addition of low glucose concentrations from 15 nM–500 nM. Even, with the addition of solutions with glucose concentrations as low as 15 nM, significantly high current response can be seen with an extremely fast response time which is lower than 1 s (Fig. 8 (b)) when compared with the response time of ~10 s for CuO nanotubes array [24] and ~2 s for CuO nanoneedles [15]. Noticeably, this very low LOD obtained from nanoporous 3D Cu_2O electrode (15 nM) is extremely lower than the results obtained for glucose detection by Cu based oxide nanomaterials, such as 670 nM for pod-like Cu_2O nanowires [17], 300 nM for CuO nanowires [22], 49 nM for CuO nanowires/Cu plate [14], 100 nM for CuO nanotube arrays [24] and 100 nM for CuO nanoneedles [15]. Also this LOD is lower than those for metallic copper and noble metal based nanomaterials such as 35 nM for copper nanowires [33], 100 nM for 3D ordered macroporous platinum template [34], 500 nM for copper nanoparticles on MWCNTs [5] and 2 μM for platinum nanoflower monolayer on a single-walled carbon nanotube membrane [35]. The superior performance shown by nanostructures grown on CF having a very low LOD and a high sensitivity is attributed to the distribution of Cu_2O nanotubes and nanorods

Table 1
Non-enzymatic glucose sensing performances of porous or 1-dimensional nanostructures.

Electrode material	Detection potential (V)	Sensitivity (μA mM^{-1} cm^{-2})	Linear Range (μM)	LOD (μM) (S/N = 3)	Electrolyte	Response time (s)	Ref.
Nanoporous Cu_2O NRs/NTs/CF	+0.4 (vs. Ag/AgCl)	5792.7	Upto 100	0.015	0.1 M NaOH	<1	This work
"	"	1002.1	575-4098.9	–	"	<1	"
Cu_2O NRs/Cu plate	+0.5 (vs. Ag/AgCl)	141.9	27-17,280	0.51	0.1 M NaOH	~5	"
3D ordered, macroporous platinum template	+0.5 (vs. SCE)	31.3	1-10,000	0.1	PBS (pH 9.18)	<2	[34]
Mesoporous 3D Cu_2O nanothorns	+0.55 (vs. Ag/AgCl)	97,900		0.005	0.1 M NaOH	–	[18]
Pod-like Cu_2O NWs	+0.5 (vs. SCE)	6680.7	1–1800	0.67	0.1 M NaOH	–	[17]
CuO NWs	+0.35 (vs. Ag/AgCl)	2217.4	1-18,800	0.3	1.0 M NaOH	–	[22]
CuO NWs/Cu plate	+0.33 (vs. Ag/AgCl)	[a]490	0.4–2000	0.049	0.15 M NaOH	<1	[14]
CuO nanoneedles	+0.6 (vs. SCE)	912.7	1-5300	0.1	0.1 M NaOH	<2	[15]
Cu NWs	+0.6 (vs. Ag/AgCl)	420.3	Upto 3000	0.035	0.05 M NaOH	–	[33]
CuO NTs array	+0.32 (vs. SCE)	1890	5-3000	0.1	1.0 M NaOH	<10	[24]

[a] - μA mM^{-1}.

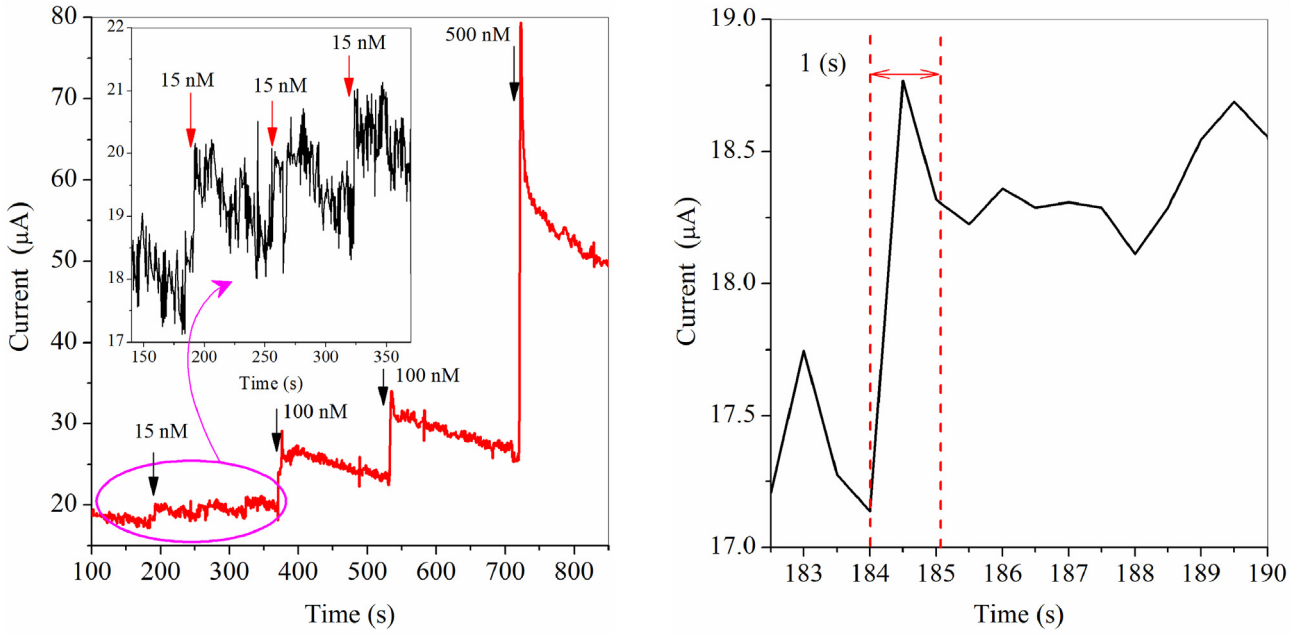

Fig. 8. Chronoamperometric measurements performed on nanoporous Cu_2O nanostructured electrode in a 0.1 M NaOH solution, (a) - at low concentrations of glucose having concentrations of 15, 100, 500 nM (e) - the enlarged amperometric response step.

grown on CF over the entire space and increased effective surface area that is present in them due to the high porosity in the surface. As a result, these nanostructures provide a higher accessibility to glucose molecules increasing the number of active sites compared to rigatoni type nanostructures grown on Cu plates.

3.4. Interference, selectivity, stability and reproducibility

Fig. 9 (a) shows the chronoamperometric responses of nanoporous 3D Cu_2O/CF and Cu_2O/Cu plate electrodes to glucose upon addition of 0.1 mM fructose, sucrose, ascorbic acid (AA), NaCl, uric acid (UA) and citric acid (CA) in 0.1 M NaOH solution at +0.4 V vs. Ag/AgCl. For a better comparison, the current response of the nanoporous 3D Cu_2O film electrode to 1 mM glucose was set at 100%, and the other electrochemical responses were normalized by the electrochemical response of 1 mM glucose on the nanoporous 3D Cu_2O film electrode (black bars) (Fig. 9 (b)). For the Cu_2O electrode, interference response from fructose, sucrose, AA, CA and UA were only 8.9, 3.9, 7.9, 3.0 and 9.0%, respectively. In addition, 0.1 mM NaCl showed a negative response of −1.0% suggesting high robustness for inactivity of the sensor for chloride ions. For further elaboration of enhanced selectivity of nanoporous 3D Cu_2O/CF electrode, the selectivity study was performed with the addition of 1.0 mM fructose, sucrose and AA, at the same time for better comparison, similar concentration of 1 mM glucose was added. As can be seen in Fig. 9 (b) (red bars), the normalized current response for 1 mM fructose, sucrose and AA were 35%, 50% and 60% respectively. This shows that the electrochemical detection of glucose by Cu_2O/CF electrode is disturbed by the presence of the interfering electroactive species. It can be stated that the higher surface area accelerates the kinetically controlled electro-oxidation reaction of glucose. In addition, the high selectivity of Cu_2O/CF electrode to glucose also proves that the oxidation of fructose, sucrose, AA, CA and UA are diffusion-controlled electrochemical processes, while the oxidation of glucose is a kinetically controlled electrochemical process. The results reveal that the *in-situ* grown

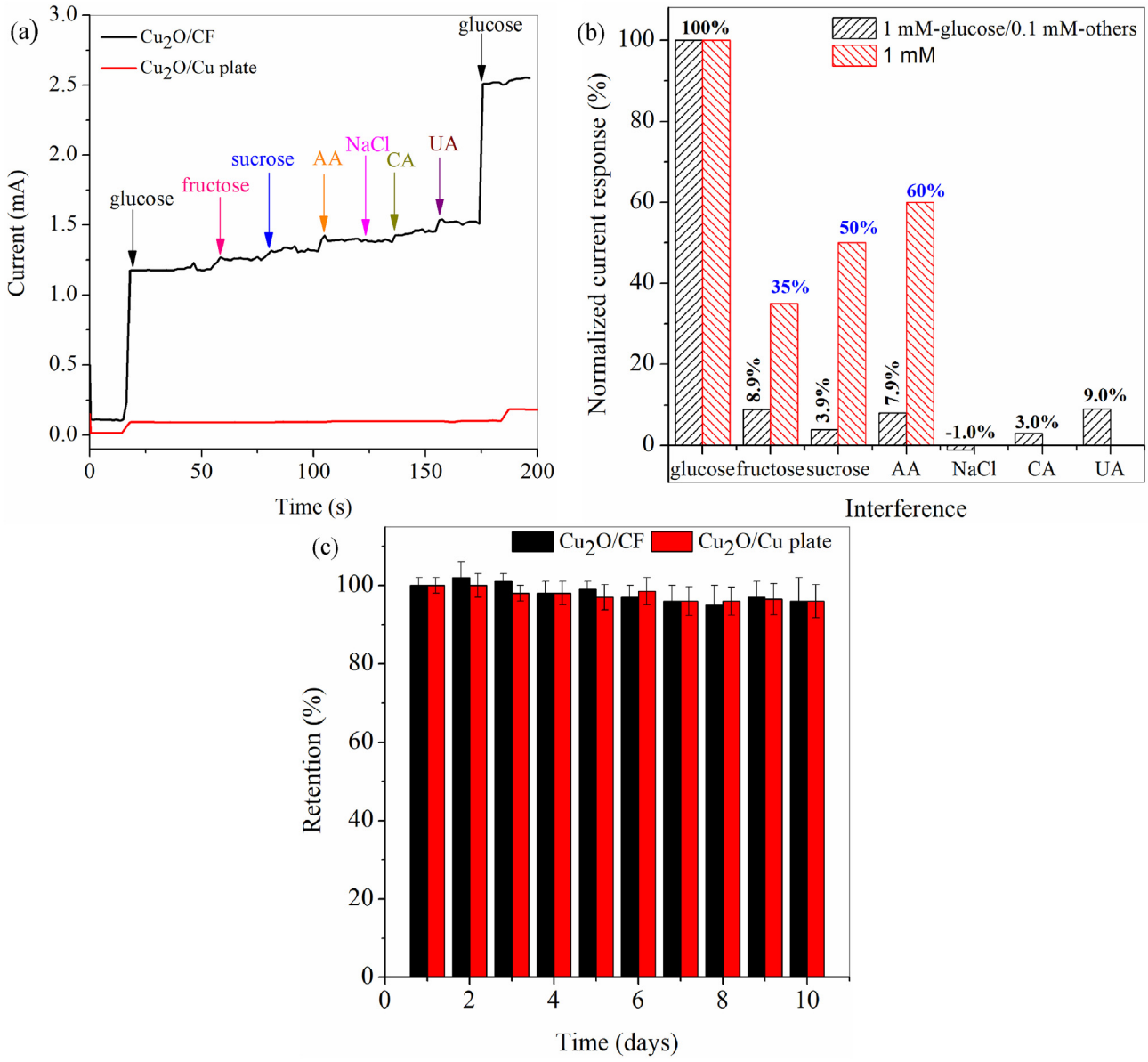

Fig. 9. Chronoamperometric response of Cu_2O/CF (black solid line) and Cu_2O/Cu plate (red solid line) electrode with successive addition of glucose (1.0 mM) and other interfering species (0.1 mM) of fructose, sucrose, ascorbic acid, NaCl, citric acid and uric acid into a 0.1 M NaOH solution at +0.4 V. (c) The long-term stability of nanoporous 3D Cu_2O/CF and Cu_2O/Cu plate electrodes over 10 days.

nanoporous Cu_2O/CF electrode provides a promising platform for fabrication of non-enzymatic glucose sensors.

The long-term stability of *in-situ* nanoporous Cu_2O/CF and Cu_2O/Cu plate electrodes over 10 days were observed with the addition of 1 mM glucose. Current response at first day was set as 100% and the current responses for 1 mM glucose of other days were normalized as shown in Fig. 9 (c). Fig. 9 (c) reveals that the current response of the Cu_2O/CF and Cu_2O/Cu plate electrodes were around 95% after 10 days suggesting this electrode exhibits good stability for oxidation of glucose. At the same time, the relative standard deviation for the reproducibility of the electrodes were measured to be 2.8% and 3%.

4. Conclusions

Electrochemically anodized $Cu(OH)_2$ nanostructures were converted to 1D Cu_2O nanostructures having highly porous nanotubes and nanorods formed on CF and grooved macaroni type structures formed on Cu plate, and employed for non-enzymatic detection of glucose. Electrochemical glucose sensing performance of 1D Cu_2O nanostructures grown on Cu foam produced excellent sensor performance with a very low detection limit and high sensitivity of 15 nM and 5792.7 $\mu A\,mM^{-1}\,cm^{-2}$ respectively and very fast response time of less than 1 s, wide detection range fitted by Langmuir isothermal theory was up to 60 mM with high sensitivity of 1565.2 $\mu A\,mM^{-1}\,cm^{-2}$. The sensitivity was ~41-fold larger than when compared with the sensitivity (141.9 $\mu A\,mM^{-1}\,cm^{-2}$) of Cu_2O nanorods formed on Cu plate. This shows that the different surface morphological properties associated with nanostructures grown on CF and Cu plates have given rise to contrasting differences in response to glucose sensing. In addition, nano-porous Cu_2O electrode had satisfactory selectivity for glucose, with no significant interference from commonly existing interfering species in blood, such as fructose, sucrose, AA, NaCl, CA and UA. Glucose response of both types of nanostructured Cu_2O film electrodes remained stable

with only a depreciation of ~5% in sensitivity during the first 10 days.

Acknowledgements

Financial assistance from the research grant (AP/3/2/2014/RG/08) of University of Colombo, Sri Lanka is gratefully acknowledged. The high-energy XRD measurements were carried out at SPring-8 with the approval of the Japan Synchrotron Radiation Research Institute (JASRI) under the proposal no 2017B1539.

Appendix A. Supplementary data

Supplementary data to this article can be found online at https://doi.org/10.1016/j.electacta.2019.135177.

References

[1] J.K. Gao Z, J. Liu, J. Chang, D. Wu, J. He, K. Wang, F. Xu, Mesocrystalline Cu2O hollow nanocubes: synthesis and application in non-enzymatic amperometric detection of hydrogen peroxide and glucose, CrystEngComm 14 (20) (2012) 6639–6646.
[2] H. Wang, Y. Liu, M. Li, H. Huang, H.M. Xu, R.J. Hong, H. Shen, Multifunctional TiO2nanowires-modified nanoparticles bilayer film for 3D dye-sensitized solar cells, Optoelectron, Adv. Mater. Rapid Commun. 4 (2010) 1166–1169.
[3] D.M. Chen X, H. Pan, H. Liu, Nonenzymatic glucose sensor based on flower-shaped Au@ Pd core–shell nanoparticles–ionic liquids composite film modified glassy carbon electrodes, Electrochim. Acta 56 (2) (2010) 636–643.
[4] Y. Song, C. Zhu, H. Li, D. Du, Y. Lin, A nonenzymatic electrochemical glucose sensor based on mesoporous Au/Pt nanodendrites, RSC Adv. 5 (2015) 82617–82622.
[5] Y.S. Wu HX, W.M. Cao, Y. Li, G. Liu, Y. Wen, H.F. Yang, In situ growth of copper nanoparticles on multiwalled carbon nanotubes and their application as non-enzymatic glucose sensor materials, Electrochim. Acta 55 (11) (2010) 3734–3740.
[6] J. Jiang, P. Zhang, Y. Liu, H. Luo, A novel non-enzymatic glucose sensor based on a Cu-nanoparticle-modified graphene edge nanoelectrode, Anal. Methods. 9 (2017) 2205–2210.
[7] A. Tarlani, M. Fallah, B. Lotfi, A. Khazraei, S. Golsanamlou, J. Muzart, M. Mirza-Aghayan, New ZnO nanostructures as non-enzymatic glucose biosensors, Biosens. Bioelectron. 67 (2015) 601–607.
[8] H.Y. Ahmad R, N. Tripathy, M.S. Ahn, K.S. Bhat, T. Mahmoudi, Y. Wang, J.Y. Yoo, D.W. Kwon, H.Y. Yang, Highly efficient non-enzymatic glucose sensor based on CuO modified vertically-grown ZnO nanorods on electrode, Sci. Rep. 7 (1) (2017) 5715.
[9] G.N. Dar, A. Umar, S.A. Zaidi, S. Baskoutas, S.H. Kim, M. Abaker, A. Al-Hajry, S.a. Al-Sayari, Fabrication of highly sensitive non-enzymatic glucose biosensor based on ZnO nanorods, Sci. Adv. Mater. 3 (2011) 901–906.
[10] T.A. Wen X, M. Long, Flake-like Cu2O on TiO2 nanotubes array as an efficient nonenzymatic H2O2 biosensor, J. Electroanal. Chem. 785 (2017) 33–39.
[11] M. Hussain, Z.H. Ibupoto, M.A. Abbasi, X. Liu, O. Nur, M. Willander, Synthesis of three dimensional nickel cobalt oxide nanoneedles on nickel foam, their characterization and glucose sensing application, Sensors 14 (2014) 5415–5425.
[12] J.Q. Lang XY, H.Y. Fu, C. Hou, G.F. Han, P. Yang, Y.B. Liu, Nanoporous gold supported cobalt oxide microelectrodes as high-performance electrochemical biosensors, Nat. Commun. 4 (2013) 2169, https://doi.org/10.1038/ncomms3169.
[13] D.J. Li C, M. Kurniawan, D. Sun, H. Tabata, Nanoporous CuO layer modified Cu electrode for high performance enzymatic and non-enzymatic glucose sensing, Nanotechnology 26 (2014) 15503, https://doi.org/10.1088/0957-4484/26/1/015503.
[14] Z. Zhuang, X. Su, H. Yuan, Q. Sun, D. Xiao, M.M.F. Choi, An improved sensitivity non-enzymatic glucose sensor based on a CuO nanowire modified Cu electrode, Analyst 133 (2008) 126–132.
[15] D. Ye, G. Liang, H. Li, J. Luo, S. Zhang, H. Chen, J. Kong, A novel nonenzymatic sensor based on CuO nanoneedle/graphene/carbon nanofiber modified electrode for probing glucose in saliva, Talanta 116 (2013) 223–230.
[16] A.-J. Wang, J.-J. Feng, Z.-H. Li, Q.-C. Liao, Z.-Z. Wang, J.-R. Chen, Solvothermal synthesis of Cu/Cu2O hollow microspheres for non-enzymatic amperometric glucose sensing, CrystEngComm 14 (4) (2012) 1289–1295.
[17] L.Z. Lu W, Y. Sun, H. Dai, P. Ni, S. Jiang, Y. Wang, Z. Li, Direct growth of pod-like Cu2O nanowire arrays on copper foam: highly sensitive and efficient nonenzymatic glucose and H2O2 biosensor, Sens. Actuators B Chem. 231 (2016) 860–866.
[18] Z.Z. Dong C, H. Zhong, T. Kou, J. Frenzel, G. Eggeler, Three-dimensional Cu foam-supported single crystalline mesoporous Cu2O nanothorn arrays for ultra-highly sensitive and efficient nonenzymatic detection of glucose, ACS Appl. Mater. Interfaces 7 (36) (2015) 20215–20223.
[19] S. a G. Evans, J.M. Elliott, L.M. Andrews, P.N. Bartlett, P.J. Doyle, G. Denuault, Detection of hydrogen peroxide at mesoporous platinum microelctrodes, Anal. CNano Energy Full paper E ffi cient charge carrier separation and excellent visible light photoresponse in Cu 2 O nanowireshem. 74 (2002) 1322–1326.
[20] M. Nur, I. Salehmin, L. Je, W.F. Mark-lee, M. Azuwa, K. Ari, M. Ha, H. Jumali, M.B. Kassim, Solar Energy Materials and Solar Cells Highly Photoactive Cu 2 O Nanowire Fi Lm Prepared with Modi Fi Ed Scalable Synthesis Method for Enhanced Photoelectrochemical Performance, vol. 182, 2018, pp. 237–245.
[21] T. Zhou, Z. Zang, J. Wei, J. Zheng, J. Hao, F. Ling, Nano Energy Full paper E ffi cient charge carrier separation and excellent visible light photoresponse in Cu 2 O nanowires, 50, 2018, pp. 118–125.
[22] Z.Z. Li Z, Y. Chen, Y. Xin, Sensitive electrochemical nonenzymatic glucose sensing based on anodized CuO nanowires on three-dimensional porous copper foam, Sci. Rep. 5 (2015) 16115.
[23] C. Yu, J. Cui, Y. Wang, H. Zheng, J. Zhang, X. Shu, J. Liu, Y. Zhang, Y. Wu, Porous HKUST-1 derived CuO/Cu2O shell wrapped Cu(OH)2 derived CuO/Cu2O core nanowire arrays for electrochemical nonenzymatic glucose sensors with ultrahigh sensitivity, Appl. Surf. Sci. 439 (2018) 11–17.
[24] L. Xu, Q. Yang, X. Liu, J. Liu, X. Sun, One-dimensional copper oxide nanotube arrays: biosensors for glucose detection, RSC Adv. 4 (2014) 1449–1455.
[25] S. Sahoo, S. Husale, B. Colwill, T. Lu, S. Nayak, P.M. Ajayan, Electric field directed self-assembly of cuprous oxide nanostructures for photon sensing, ACS Nano 3 (2009) 3935–3944.
[26] W. Wang, O.K. Varghese, C. Ruan, M. Paulose, C.A. Grimes, Synthesis of CuO and Cu2O crystalline nanowires using Cu(OH)2 nanowire templates, J. Mater. Res. 18 (2003) 2756–2759.
[27] Y. Tan, X. Xue, Q. Peng, H. Zhao, T. Wang, Controllable fabrication and electrical performance of single crystalline Cu2O nanowires with, High Aspect Ratios 7 (2007) 3723–3728.
[28] G.A. Felix S, P. Kollu, B.P. Raghupathy, S.K. Jeong, Electrocatalytic activity of Cu2O nanocubes based electrode for glucose oxidation, J. Chem. Sci. 126 (2014) 25–32.
[29] Q. Zhang, Q. Luo, Z. Qin, L. Liu, Z. Wu, B. Shen, W. Hu, Self-assembly of graphene-encapsulated Cu composites for nonenzymatic glucose sensing, ACS Omega 3 (2018) 3420–3428.
[30] K.T. Marioli JM, Electrochemical characterization of carbohydrate oxidation at copper electrodes, Electrochim. Acta 37 (1992) 1187–1197.
[31] and H.Z. Qianyi Gong, Li-Ping Sun, Zhouling Wu, Li-Hua Huo, Enhanced non-enzymatic glucose sensing of Cu − BTC- derived porous copper @ carbon agglomerate, J. Mater. Sci. (2018), https://doi.org/10.1007/s10853-018-2078-x.
[32] L.S. Li Y, Y. Zhong, Y. Zhang, W. Weng, Carbon quantum dots/octahedral Cu2O nanocomposites for non-enzymatic glucose and hydrogen peroxide amperometric sensor, Sens. Actuators B Chem. 206 (2015) 735–743.
[33] Y. Zhang, L. Su, D. Manuzzi, H. Valdés, E.D.L. Monteros, W. Jia, D. Huo, C. Hou, Y. Lei, Ultrasensitive and selective non-enzymatic glucose detection using copper nanowires, Biosens. Bioelectron. 31 (2012) 426–432.
[34] Y. Song, D. Zhang, W. Gao, X. Xia, Nonenzymatic glucose detection by using a three-dimensionally ordered, macroporous platinum template, Chem. Eur J. 11 (2005) 2177–2182.
[35] L. Su, W. Jia, L. Zhang, C. Beacham, H. Zhang, Y. Lei, Facile synthesis of a platinum nanoflower monolayer on a single-walled carbon nanotube membrane and its application in glucose detection, J. Phys. Chem. C 114 (2010) 18121–18125.